



Scholars' Mine

Masters Theses

Student Theses and Dissertations

1968

Estimation of film boiling heat transfer coefficients for cylindrical heaters in corresponding states fluids

Gary Joseph Capone

Follow this and additional works at: https://scholarsmine.mst.edu/masters_theses

 Part of the [Chemical Engineering Commons](#)

Department:

Recommended Citation

Capone, Gary Joseph, "Estimation of film boiling heat transfer coefficients for cylindrical heaters in corresponding states fluids" (1968). *Masters Theses*. 5298.

https://scholarsmine.mst.edu/masters_theses/5298

This thesis is brought to you by Scholars' Mine, a service of the Missouri S&T Library and Learning Resources. This work is protected by U. S. Copyright Law. Unauthorized use including reproduction for redistribution requires the permission of the copyright holder. For more information, please contact scholarsmine@mst.edu.

ESTIMATION OF FILM BOILING HEAT TRANSFER COEFFICIENTS FOR
CYLINDRICAL HEATERS IN CORRESPONDING STATES FLUIDS

BY

GARY JOSEPH CAPONE ,

A

THESIS

submitted to the faculty of

THE UNIVERSITY OF MISSOURI - ROLLA

in partial fulfillment of the requirements for the

Degree of

MASTER OF SCIENCE IN CHEMICAL ENGINEERING

Rolla, Missouri

1968

Approved by

E. H. Park

(advisor)

Orin K. Crosser

Virgil J. Flanagan

TABLE OF CONTENTS

	Page
Abstract	iii
Acknowledgements	iv
List of Illustrations.	v
List of Tables	vi
CHAPTER	
I. Introduction.	1
II. Previous Work	4
III. Film Boiling of Corresponding States Fluids	10
IV. Experimental Equipment.	13
V. Experimental Procedure.	17
VI. Results	19
VII. Discussion of Results	24
VIII. Conclusions	33
Nomenclature	35
Bibliography	37
Appendices	39
A. Discussion of Errors.	40
B. Sample Calculations	41
C. Calculated Data	44
D. Operating Conditions.	53
Vita	55

ABSTRACT

An investigation of film boiling heat transfer was made with cylindrical heaters. The (0.75" O.D.) gold plated, copper heaters were positioned horizontally in pools of liquid argon, nitrogen, and carbon monoxide.

A correlation for film boiling corresponding states fluids is derived and discussed. The correlation is a least squares fit of three variables: the diameter of the cylindrical heater, the reduced pressure of the system, and the temperature difference between the heater surface and the saturated pool.

ACKNOWLEDGEMENTS

The author wishes to express his appreciation to his advisor,
Dr. E. L. Park.

The author acknowledges the financial assistance of the
National Science Foundation.

The technical assistance of Mr. Craig Jöhler, Mr. Robert
Montgomery, and Mr. Dave Porchey is also appreciated.

The financial and moral assistance of my parents and brother
will always be remembered.

LIST OF ILLUSTRATIONS

Figure	Page
1. A Typical Boiling Heat Transfer Curve	2
2. Heat Transfer Element	14
3. Pressure and Condensing System - Schematic Diagram.	16
4. Film Boiling of Liquid Nitrogen, 0.75 in. Diameter Heater .	20
5. Film Boiling of Liquid Argon, 0.75 in. Diameter Heater. . .	21
6. Film Boiling of Liquid Carbon Monoxide, 0.75 in. Diameter Heater.	22
7. Comparison of Film Data with Bromley's Correlation.	30
8. Comparison of Film Data with Breen and Westwater's Correlation	32

LIST OF TABLES

	Page
I. Error Analysis of Experimental Data	27
II. Flanigan Ph.D. Thesis - Nitrogen and Argon Data	45
III. Park Ph.D. Thesis - Nitrogen Data	47
IV. Sciance Ph.D. Thesis - Methane Data	48
V. Capone Nitrogen Data - 0.75" O. D. Heater	49
VI. Operating Conditions.	54

CHAPTER I

INTRODUCTION

This investigation studied the film boiling of corresponding states fluids from a horizontal cylinder. In Figure 1, is shown the typical boiling curve as presented by Nukiyama (12) in 1934. The curve is a plot of the logarithm of the heat flux from the heating surface as a function of the logarithm of the temperature difference between the surface and the saturated fluid.

The curve is divided into four distinct regions. Initially, the temperature difference is small and a small heat flux is obtained. This region of small temperature difference is the convection region of the boiling curve and the heat is carried away by the convective currents in the liquid. As the temperature difference is increased, the heat flux increases to a point where bubbles form at specific sites called nuclei. The point where bubbles initially form is the beginning of the nucleate boiling region. The number of bubbles formed will increase with increasing temperature difference until point A is reached. Point A in Figure 1 is known as the burnout point and is characterized by the formation of vapor film over the heat transfer surface. At this point in the boiling curve, the very high heat transfer rate in the nucleate boiling region decreases because of the vapor formation. The third region is known as the unstable film boiling region. In this region a film is continuously forming and collapsing as the temperature difference increases and the heat transferred decreases because of the partial vapor film. The next critical point reached is the Leindenfrost Point. This point is attained when a stable film of

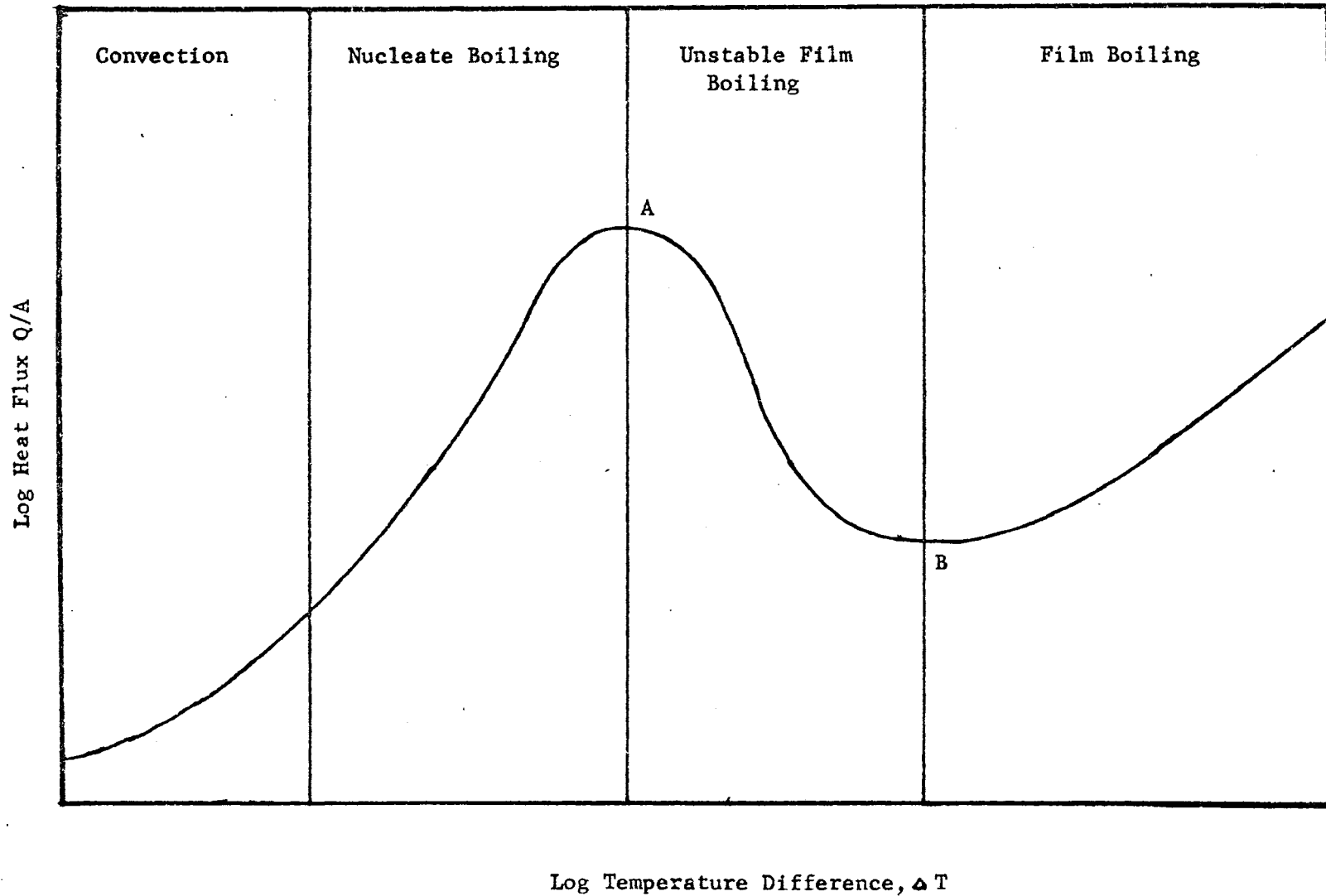


Figure 1 A Typical Boiling Heat Transfer Curve

vapor is formed over the entire surface. As the temperature difference is increased further, the fourth region is entered. This region of film boiling is investigated in the following dissertation.

CHAPTER II

PREVIOUS WORK

Scorah and Farber (7) described the entire boiling curve (Figure 1) by boiling water from nickel, tungsten, chromel A, and chromel C wires. They found the boiling curve to depend on the pressure of the system and the metal used for the heat transfer element.

Bromley (4) suggested an analysis for film boiling similar to Nusselt's (10) development for condensation. As a result of visual observations, he assumed a mechanism in which the vapor film is in dynamic equilibrium with the surrounding liquid. As the vapor rises under the action of bouyant forces, vapor is added to the film from the surrounding liquid. The resulting equation is given below. All the symbols in the following equations are defined on page 35.

$$h = (\text{const}) \left[\frac{k_v \rho_v (\rho_l - \rho_v) g \lambda'' c_p}{D \Delta T P_r} \right]^{\frac{1}{4}} \quad (1)$$

The value of the constant was found experimentally to be 0.62. This value is the arithmetic average value between 0.512 and 0.724, which are the values predicted by Bromley (4) by assuming the surrounding liquid is either stagnant, or moving freely with the vapor.

Bromley (4) found the heat transfer coefficient to be independent of the heater material and that the dependence of heat transfer on the pressure of the system can be calculated from the pressure effect on the physical properties of the system. Bromley's data also showed that the heat transfer coefficient varies inversely with the heater diameter in the range of 0.188 inches to 0.466 inches. Bromley (5) improved his film boiling correlation by using a λ'' corrected for the sensible heat of the vapor:

$$\lambda'' = \lambda[1.0 + (0.34 c_p \Delta T) / \lambda]^2 \quad (2)$$

Banchero, Barker, and Boll (2) boiled liquid oxygen with heaters of various diameters to show the limitations of Bromley's equation. They found that Bromley's equation predicts the effect of diameter when in the range of 0.069 to 0.127 inches, but fails to predict the effect of diameter when a range of 0.025 to 0.75 inches is considered. These authors present the following equation as a modification of Bromley's equation (1).

$$\begin{aligned} h &= a(1.0/D + C)F^{1/2} \\ C &= \text{constant } (36.5 \text{ in}^{-1}) \\ F &= \left[\frac{k^3 \rho_v \lambda' (\rho_l - \rho_v) g}{\Delta T u_v} \right]^{1/2} \end{aligned} \quad (3)$$

Both a and C are determined by a trial and error fit of experimental data. Their investigation showed the heat transfer coefficient to vary inversely with the diameter of the heater and to increase with increasing pressure.

Chang (6) chose to analyze film boiling by considering hydrodynamic wave formation. The vapor film will grow with increasing heat flux until the vapor breaks the vapor-liquid interface at intervals equal to the critical wavelength, l_{cr} ,

where:

$$l_{cr} = 2\pi \left[\frac{\sigma}{g(\rho_l - \rho_v)} \right]^{1/2} \quad (4)$$

Chang's final equation is

$$(Nu_1') = 0.234 (P_r * G_r *)^{1/3} \quad (5)$$

where:

$$P_R^* = v/a_c, \quad G_R^* = \frac{g\rho_V^2 L^3 (\rho_l - \rho_V)}{u_V^3 \rho_V}$$

$$a_c = \frac{k_V \theta_V}{2\rho_V}, \quad \theta_V = T_{sat} - T_V$$

Chang (6) concluded that the heat transfer coefficient will increase with increasing pressure and that the effect of temperature and pressure can be calculated by its effect on the physical properties of the liquid and its vapor. Also, he found that the first stage of wave motion development is governed by hydrodynamic effects. In this stage where hydrodynamic effects are important, the vapor film surrounding the heat transfer surface is very thin, but the vapor film will continue to grow. The film thickness will increase to the extent that the heat being transferred will decrease. The wavelength of the standing wave at the vapor-liquid interface is longer than the critical wavelength given by equation 4. Because of the hydrodynamic forces, the interface will break and vapor bubbles will be released. The film thickness will be reduced and an equilibrium condition will be established. Since the vapor will be periodically released at the interface, an average film thickness will be maintained and the heat transfer is now governed by conduction through the vapor.

Berenson (1) used a similar analysis of hydrodynamic instability in the development of a correlation for film boiling on a horizontal surface. The final equation is

$$h = 0.425 \left[\frac{k_V^3 \rho_V g (\rho_l - \rho_V) \lambda}{u_V \Delta T (g_c / (\rho_l - \rho_V))^{1/2}} \right]^{1/2} \quad (6)$$

Equation 6 is similar to Bromley's (equation 1) in that substitution of $(g_c/g(\rho_1-\rho_v))^{1/2}$ for D in equation 1 will give equation 6. Berenson's equation seems to be effective only near the minimum point of the film boiling region.

Breen and Westwater (3) investigated film boiling of Freon 113 and Isopropanol from horizontal cylinders ranging in diameter from 0.185 to 1.895 inches. They attempted to develop an equation that would predict the effects of diameter in the film boiling regime based on hydrodynamics and Taylor instability. Their study suggested that there are two mechanisms controlling film boiling. These mechanisms are a function of "the most dangerous wavelength" λ_d ,

where:

$$\lambda_d = \sqrt{3}\lambda_c$$

$$\begin{aligned}\lambda_c &= \text{the critical wavelength} \\ &= 2\pi(g_c\sigma/g(\rho_1-\rho_v))^{1/2}\end{aligned}$$

The Breen and Westwater correlation is

$$h(\lambda_c)^{3/4}/F = 0.59 + 0.069\lambda_c/D \quad (7)$$

where:

$$F = \left[\frac{k_v^3 \rho_v (\rho_1 - \rho_v) g \lambda_c'}{u_v \Delta T} \right]^{1/4}$$

Breen and Westwater (3) found that there was a certain regime of λ_c/D which fit Bromley's data. Accordingly, they suggested an alternative procedure involving three boiling regions.

One of the boiling regions is

$$\lambda_c/D < 0.8 ; h(\lambda_c)^{3/4}/F = 0.60$$

The above condition develops when the diameter of the cylinder is very large and wave motion appears around the perimeter of the cylinder. In this region surface tension effects are important.

The next boiling region is

$$0.80 < \lambda_c/D < 8 ; h(\lambda_c)^{1/4}/F = 0.62$$

In this region the surface tension effects are not important and the mechanism is determined by conduction through vapor in viscous flow. The wave formation is one dimensional at the top of the cylinder.

The third boiling region is

$$0.80 < \lambda_c/D ; h(\lambda_c)^{1/4}/F = 0.16(\lambda_c/D)^{0.83}$$

In this region of boiling the diameter of the cylinder is small and the boiling mechanism is governed by bubble release. Again, surface tension is important.

Park (13) showed the Breen and Westwater correlation (equation 7) to be inadequate in predicting the heat transferred in the film boiling of nitrogen and methane from a horizontal cylinder (0.8022" O.D.) over a wide pressure range. He found the Breen and Westwater correlation (equation 7) to be in error by +30% and -40% in predicting heat transfer coefficients when boiling methane and nitrogen, respectively. Also, his data showed a temperature dependence at high temperature differences that is not predicted by the Breen and Westwater correlation. Park's data revealed a decrease in the heat flux as the critical pressure is approached. The effect was noticed at reduced pressures greater than 0.90.

Sciencie (16), who continued Park's work, did not observe the same decrease in heat transfer at reduced pressures up to 0.90.

Flannigan (8) used his experimental data to show the correlations of Bromley (4), and Breen and Westwater (3) to be inadequate in predicting heat fluxes from cylindrical heaters boiling in nitrogen and argon. Bromley's correlation (equation 1) and the Breen and Westwater correlation (equation 7) predicted heat transfer coefficients which were approximately 55% and 50% lower than the experimental values obtained by Flannigan (8). He used a modified form of Banchemo, Barker, and Boll (2) to fit his data:

$$h = a_2(1.0/D + C)P_r^{\frac{1}{2}} \quad (8)$$

where:

$$a_2 = b_1 + b_2T_r + b_3T_r^2 + b_4T_r^3$$

$b_1 \dots b_4$ = constants in third order equation for "a",

$$C = 36.5 \text{ in}^{-1},$$

P_r = reduced pressure of the system.

The use of corresponding states fluids allowed Flannigan to substitute the reduced properties of the system for the physical properties in previous correlations. He found that using this principle of corresponding states he could predict his film boiling heat transfer coefficients within $\pm 20\%$ deviation.

CHAPTER III

FILM BOILING OF CORRESPONDING STATES FLUIDS

All of the correlation forms presented in Chapter II represent heat transfer coefficients as a function of essentially three variables. These three variables are the diameter of the heat transfer surface, the temperature difference between the surface of the heating element and the fluid, and the properties of the fluid under boiling conditions. The heat transfer coefficient can be represented functionally as follows:

$$h = f(\Delta T, D, \text{Properties of Fluid}) \quad (9)$$

By using corresponding states fluids, the properties of the fluid can be represented by some reduced property of the system. Both Pitzer (15) and Guggenheim (9) develop the following form.

$$P/P_c = f(T/T_c, V/V_c) \quad (10)$$

In this development five assumptions were made. First, Classical statistical mechanics would be used. Second, the molecules of the fluid are spherically symmetrical or they have rapid and free rotation. Third, the intramolecular vibrations are the same in the liquid and the vapor states. Fourth, the potential energy is a function only of the various intermolecular distances. Fifth, the potential energy for a pair of molecules can be written $E = A\phi(R/R_0)$ where R is the intermolecular distance, A and R_0 are constants, and ϕ is a universal function.

Pitzer (15) shows that in terms of reduced temperatures (T/T_c), volumes (V/V_c), and pressures (P/P_c) argon, krypton, and xenon behave the same. Guggenheim (9) extended Pitzer's work and found that oxygen

and nitrogen followed the principle accurately, while carbon monoxide and methane did so with slightly less accuracy. A table for comparison is given by Guggenheim (9).

Applying this principle of corresponding states, the heat transfer coefficient becomes a function of the diameter of the cylinder, the temperature difference between the heater surface and the fluid, and a reduced property of the fluid at the conditions of the system. All the properties of the system have now been replaced by a reduced property:

$$h = f(D, \Delta T, Pr) \quad (11)$$

The characterization of the fluid properties with the reduced pressure in film boiling heat transfer was introduced by Flanigan (8). Additional data for the film boiling of nitrogen, argon, and carbon monoxide are provided in this investigation in order to obtain a more complete test of the ideas of Flanigan (8), and to extend his work to another corresponding states fluid (CO). Also, the data of this investigation will further the study of surface, pressure, and diameter effects in film boiling heat transfer. As shown in Chapter II, previous correlations take the form of empirical modifications of Nusselt's (10) condensation theory. As will be shown in Chapter VII, these correlations do not accurately predict (within 30 to 80%) film boiling heat transfer coefficients for corresponding states fluids, the correlations are often limited to a small diameter range, and the correlations do not predict the effects of the system pressure in the film boiling region. Also in Chapter VII of this investigation, an empirical correlation for predicting film boiling heat transfer coefficients

is presented, and the correlation is justified by the parametric behavior of experimental data.

CHAPTER IV

DESCRIPTION OF THE EXPERIMENTAL EQUIPMENT

The equipment used in this investigation of film boiling of corresponding states fluids was a pressure vessel, two digital voltmeters, an ammeter, a power source, a pressure gauge, and a heat transfer element.

The heat transfer element (Figure 2) had a 0.40 inch O.D. Lavatite core, which was threaded with 18 threads per inch. Tungsten wire (26 gauge) was wound on the core and was secured at each end of the core by a type 4-40 screw. The core was then cemented into a copper tube with Sauereisen Electrical Resistor Cement, No. 7. Additional cement was used on both ends of the heat transfer element to reduce end losses. The heater surface was gold plated to assure negligible surface changes during nucleate boiling experiments which were performed before each film boiling experiment.

The power was supplied by a Nobatron, DCR 60-40A, 60 volt, 40 amp, Sorensen D. C. Power Source, and measured with a United Systems Corporation, Model 201, Digital D. C. voltmeter and a Weston Model I (Class 50) ammeter.

The pressure vessel was a one gallon autoclave, 5 inches I.D., twelve inches deep, and was manufactured by Autoclave Engineers, Inc. The autoclave had two windows, 3 inches thick, 2 inches in diameter, and 180° apart. The autoclave was raised and lowered pneumatically to meet the top flange which had openings for a vent plug, power leads, fill line, cooling coil entrance and exit, and a gland (Conax MHM-062-A160T with a teflon sealant) for insertion of copper-constantan thermocouples.

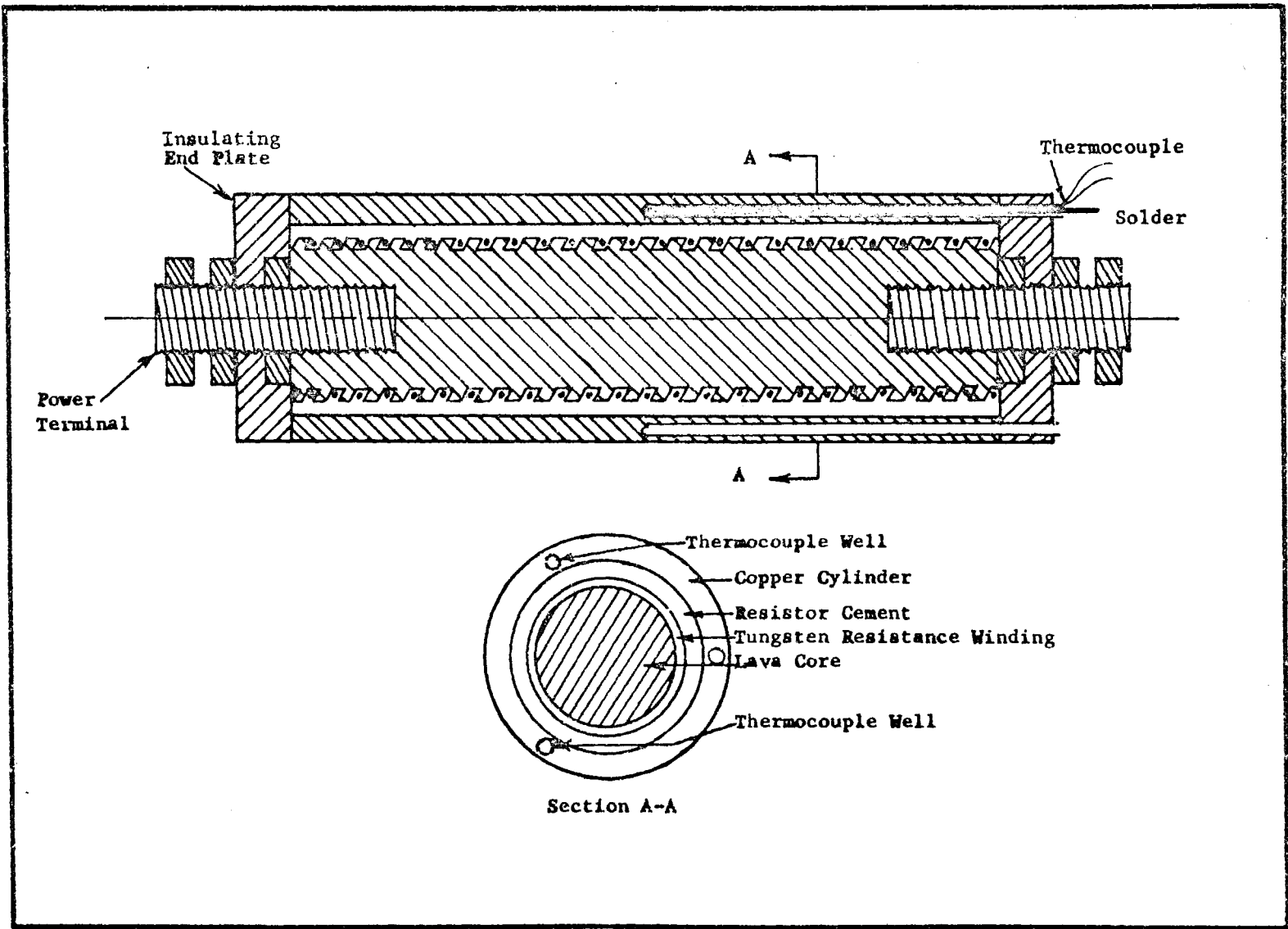


Figure 2. Heat Transfer Element

The pressure in the autoclave was controlled by passing liquid nitrogen through internal cooling coils (Figure 3). The liquid nitrogen was obtained from Linde in 110 liter, high pressure (235 psig) dewars.

The pressure in the autoclave was measured with a Heise Bourdon tube pressure gauge which had a 16 inch dial, a range from 0 to 1000 psi in 1 psi increments, and an accuracy of ± 1 psi. All the connections and fittings were sealed using Teflon tape. The tubing was 316 stainless steel, 1/4 inch O. D., and 0.065 inch wall thickness. The valves were Whitey No. 1 Series 0.25 inch (number IRS4-316).

The 24 gauge copper-constantan thermocouples were brought from the top of the autoclave to a liquid nitrogen reference junction, which was located outside the autoclave. From the reference junction the thermocouples were connected to a Leads and Northrup rotary thermocouple switch. The temperature was read with a United Systems Corporation, Model 451, Digitec, 0 to 10 m.v. millivoltmeter. In addition to the three thermocouples used for measuring the temperature of the heater surface, there was a thermocouple used to read the pool temperature. As shown in Appendix A, the instrumentation used in this investigation would permit a maximum possible scatter of less than 9% when the data are plotted as the heat flux (Q/A) versus the temperature difference (ΔT) between the surface of the heat transfer element and the fluid.

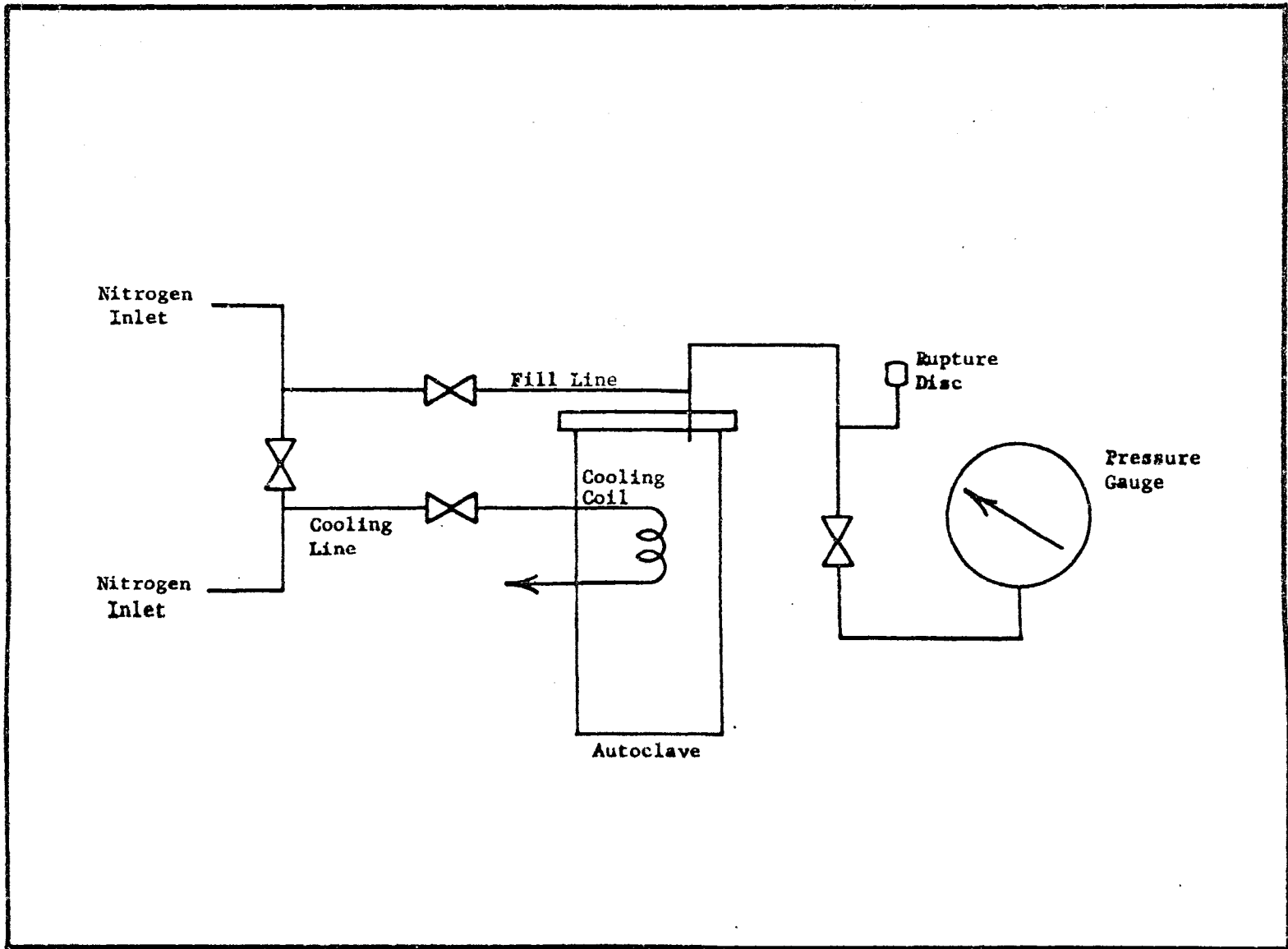


Figure 3. Pressure and Condensing System - Schematic Diagram

CHAPTER V

EXPERIMENTAL PROCEDURE

The cylindrical heat transfer element was horizontally suspended from the two power leads entering the top flange of the autoclave. The autoclave was then pneumatically raised and secured into position. The system was pressurized to check for any leakage and the liquid nitrogen reference thermos bottle was filled to ensure proper thermocouple operation. This same procedure was followed for the nitrogen, argon, and carbon monoxide runs.

When liquid nitrogen was used as the boiling media, the autoclave was filled by pouring liquid nitrogen at atmospheric pressure into the vent hole in the top flange. At the same time high pressure liquid nitrogen (235 psig) was allowed to flow through the internal cooling coils. When the liquid level was above the sight glass in the autoclave, the vent plug was placed in the vent hole and tightened. The proper nitrogen flow rate through the cooling coils was then maintained to assure the desired operating pressure. In order to achieve the saturation temperature at the desired pressure, power was supplied to the heater and the liquid was allowed to boil until the saturation temperature was reached.

During each test run, both nucleate and film boiling data were taken. The nucleate boiling data was analyzed by Mr. Craig Jöhler (11). After burnout was achieved, the film boiling data was taken. Nucleate and film boiling data were taken at six different pressures up to and including a reduced pressure of 0.95. During a given pressure run, the three thermocouples in the heater wall were constantly

monitored to ensure steady state operation before each reading. At the same time the pool temperature was recorded to ensure saturation of the liquid and the level of liquid in the autoclave was constantly observed to ensure the proper liquid level above the heater.

The same procedure was followed when boiling liquid argon or carbon monoxide. The only exception was the procedure followed in filling the autoclave. For both argon and carbon monoxide the vent plug was left secured in position at all times. The fluid in the gaseous state entered the autoclave through the fill line at a pressure of approximately 60 psig, which was controlled by a regulator on a cylinder of either argon or carbon monoxide. High pressure liquid nitrogen was passed through the coiling coils of the autoclave and maintained at a rate to keep the autoclave pressure below 60 psig. The argon or carbon monoxide were allowed to condense until the level in the autoclave was above the sight glass. The fill line was closed and a pressure run could be made.

After taking data at the full range of pressures, the fill line was opened and the liquid in the autoclave was bled to the atmosphere.

In each case, reproducibility was determined by repeated measurements of the boiling curve at an intermediate pressure.

CHAPTER VI

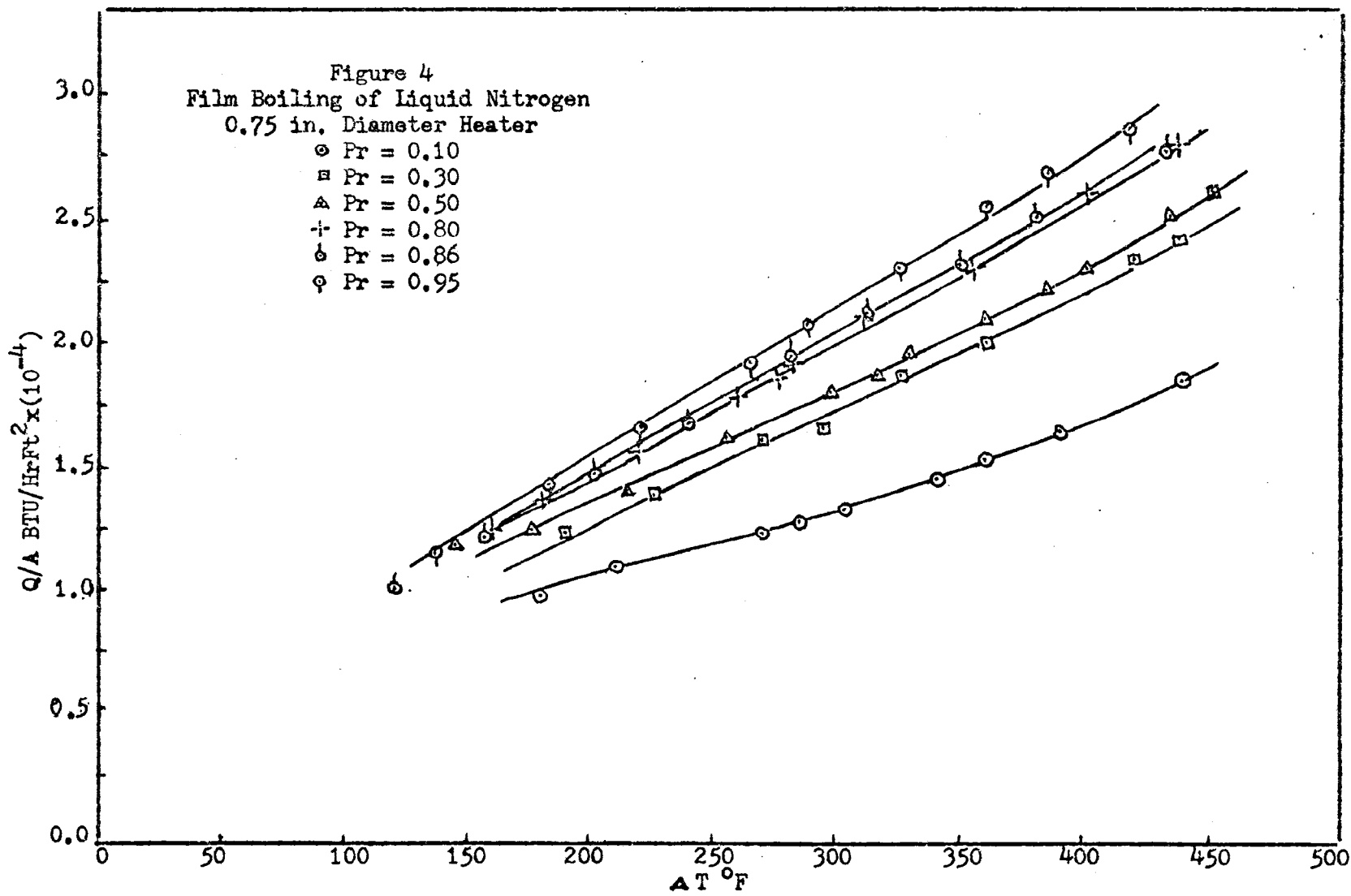
RESULTS

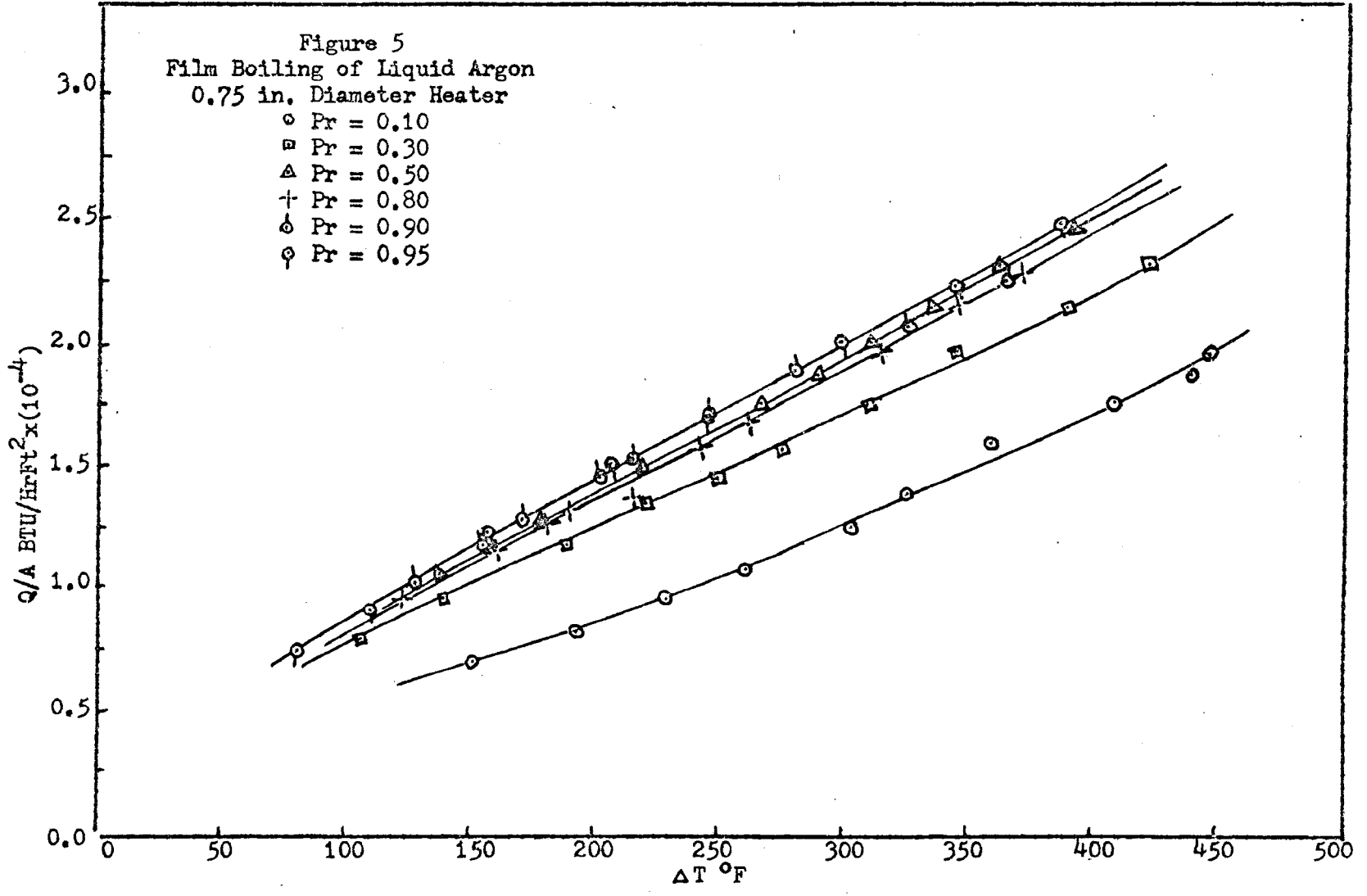
The experimental results of the investigation of film boiling heat transfer are represented by Figures 4 and 6. Liquid nitrogen, argon, and carbon monoxide were boiled from horizontal 0.75 inch diameter heaters at temperature differences of approximately 100 to 500°F between the wall temperature of the heater and the saturation temperature of the liquid. Each fluid was boiled at six pressures which included reduced pressures of 0.1 to 0.95.

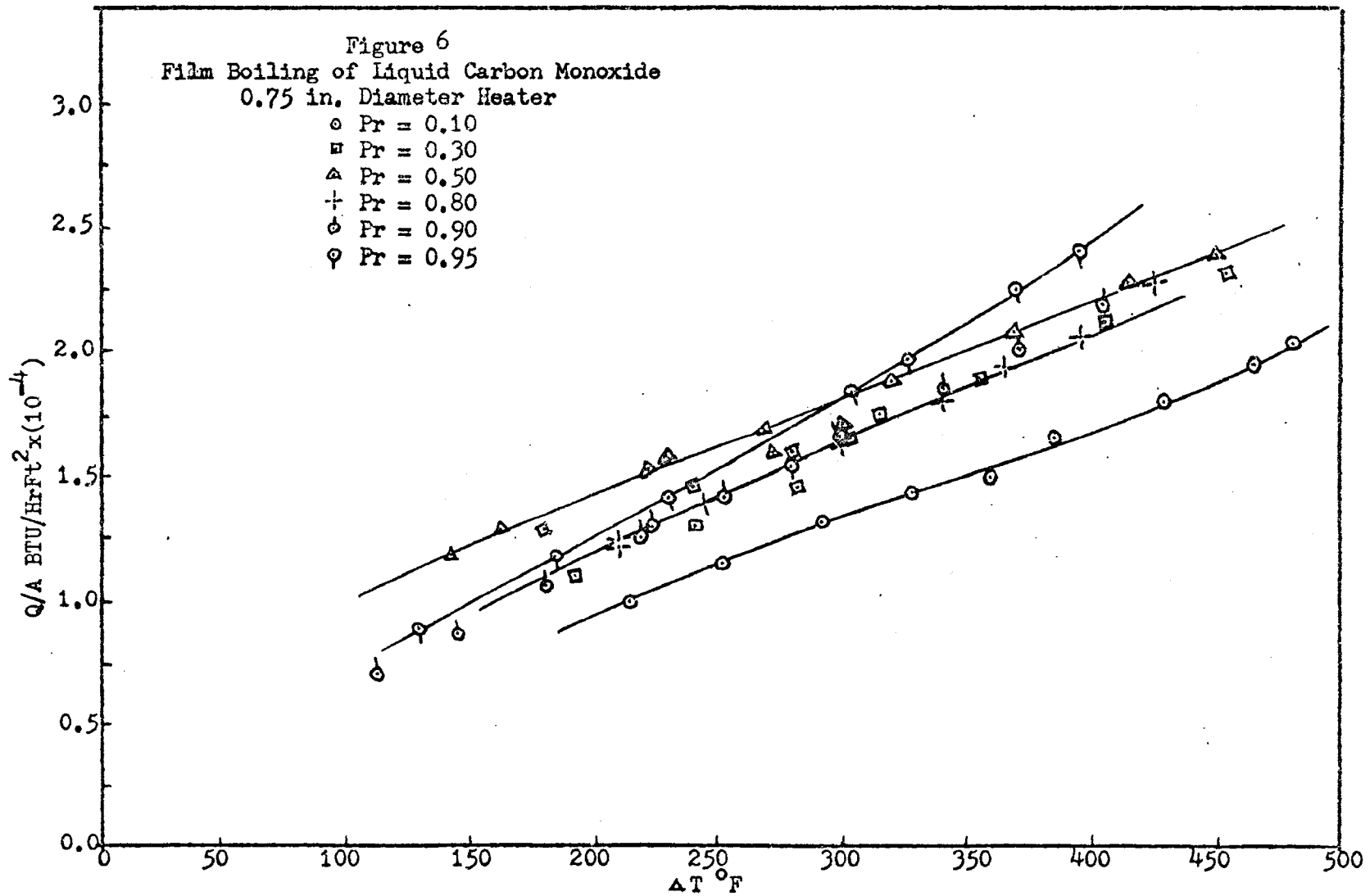
The data are plotted as the heat flux, Q/A , versus the temperature difference between the heater wall and the saturation temperature of the fluid, ΔT . In general, an increase in temperature difference results in an increase in heat flux. As shown in Figures 4 and 5, an increase in pressure at a given temperature difference will cause an increase in the heat flux for both nitrogen and argon. The data presented in Figure 6 show the same increase in heat flux with pressure for the film boiling of carbon monoxide up to a reduced pressure of 0.8, and decreases from 0.8 to 0.9. Also, the slope of the pressure curves increases at reduced pressures of 0.9 and 0.95.

The data that was obtained in order to show the reproducibility are also plotted in Figures 4 and 6, and show the maximum deviation to be less than 3%. This deviation is significantly less than the maximum relative error of 9% calculated from the measurement precision.

Three heat transfer elements were used in obtaining the data represented in Figures 4 through 6. Although the heat transfer







surfaces were shown by Johler (11) to behave differently when in the nucleate boiling region, surface effects did not appear in the film boiling region and the reproducibility of the data (the maximum experimental deviation) was again less than 3%.

CHAPTER VII

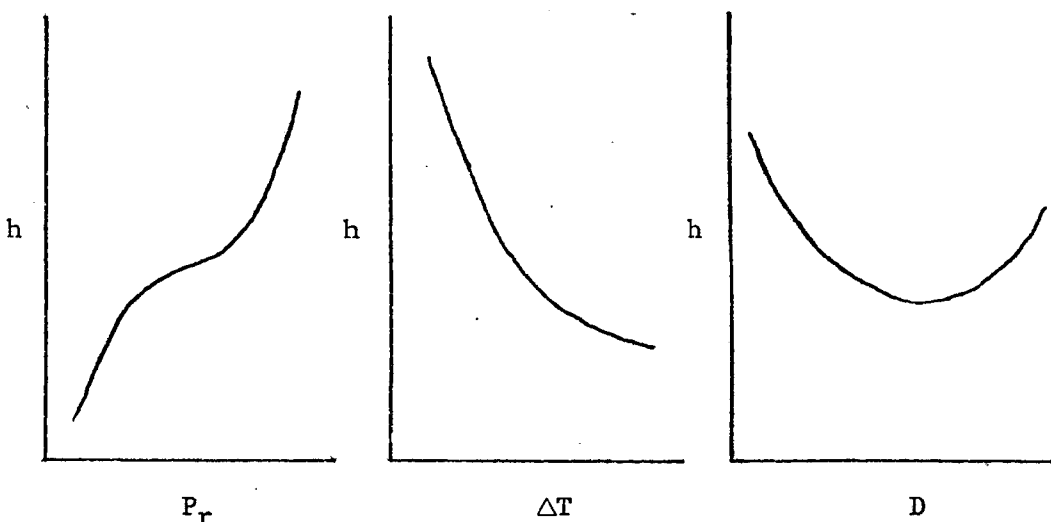
DISCUSSION OF RESULTS

All data used in this analysis were from the investigations of Flanigan (8), Park (13), Science (16), and this investigation. In all these investigations, electrically heated copper cylinders and gold plated cylinders were used. The cylinders ranged in diameter from 0.55 to 0.95 inches in diameter. The cylinders were located horizontally in a pool of a corresponding states fluid (N_2 , A_r , CH_4 , CO) and boiled under pressures ranging from 0.1 to 0.955 of the critical pressure of the fluid.

By definition, the heat transfer coefficient is the rate of heat being transferred per unit area divided by the temperature difference between the surface of the element and the boiling liquid. Therefore, the heat transfer coefficient should be some function of the diameter of the cylinder and the temperature difference. In order to obtain a more general correlation, the variation of the heat being transferred because of the system pressure must be included. The use of corresponding states fluids allows the heat transfer coefficient to be correlated as a function of the reduced pressure of the system. This theory assumes that at a given reduced pressure N_2 , A_r , CH_4 , and CO will behave similarly in the film boiling region. The heat transfer coefficient is a function of three variables in which the reduced pressure represents the influence of the physical properties of the fluid as given below;

$$h = f(\Delta T, D, P_r)$$

An empirically determined functional form of these three variables was chosen. Suggestions about the functional behavior are available from Flanigan's (8) data. His experimental heat transfer coefficients were plotted against ΔT , D , and P_r while holding the other two parameters constant. The general form of the curves are as follows:



The reduced pressure ranged from 0.1 to 0.953, the temperature difference ranged from 110 to 350°F, and the outside diameters of the cylinders were 0.55, 0.75, and 0.95 inches. The data show that h varied as a cubic with P_r , a quadratic with ΔT , and a quadratic with D . Therefore, the following expression was chosen:

$$h = a_0 + a_1(P_r) + a_2(P_r)^2 + a_3(P_r)^3 + a_4(\Delta T) + a_5(\Delta T)^2 + a_6(D) + a_7(D)^2 \quad (12)$$

Any attempt to increase the powers of the three variables in order to achieve greater accuracy can not be justified in view of the experimental data.

There were 99 data points used for the least squares curve fit and covered the entire range of D , ΔT , and P_r for both liquid nitrogen and liquid argon. The following equation is the least squares

curve fit obtained:

$$h = 255.83 + 94.69(P_r) - 86.79(P_r)^2 + 21.02(P_r)^3 - 0.3158(\Delta T) + 4.13 \times 10^{-4}(\Delta T)^2 - 438.02(D) + 286.09(D)^2 \quad (13)$$

This curve fit was then checked with additional data chosen at random from Flanigan (8), and from the data of Park (13), Sciencie (16), and this investigation. Tables (II) through (V) are the tabulated values of the independent variables (ΔT , D , P_r) and both the experimental and predicted dependent variable (h). Also in these tables are listed the percent deviations of the predicted values from the experimental values. A summary of the accuracy of equation (13) in predicting heat transfer coefficients for corresponding states fluids from horizontally positioned cylindrical heaters is presented in Table (I).

Table (I) shows the proposed least squares expression (equation 13) of Flanigan's (8) data to be acceptable. The mean percent deviation for argon and nitrogen was + 1.51% and + 0.37%, and the standard deviations being $\pm 12.30\%$ and $\pm 9.09\%$, respectively. From this same table the upper and lower bounds on the error in the prediction of h for the data of this investigation are set by the nitrogen and carbon monoxide data. For the nitrogen data the addition of the mean (8.15%) and the standard deviation (5.55%) yields the upper limit of + 13.70%. For the carbon monoxide data the addition of the mean (-3.67%) and the standard deviation (- 12.30%) yields the lower limit (- 15.97%). The limits of the argon data fall between the values for nitrogen and carbon monoxide. As shown in the table (I), the data of Park (13) and Sciencie (16) follow the equation less accurately.

Figure (4) in the Chapter VI shows that the heat flux in nitrogen increases with increasing pressure at a given temperature. If

Table I

Error Analysis of Experimental Data

<u>Investigator</u>	<u>Argon</u>	<u>Nitrogen</u>	<u>Carbon Monoxide</u>	<u>Methane</u>	
Capone	Mean Value	+3.32%	+8.15%	-3.67%	
	Standard Deviation	±8.81%	±5.55%	±12.30%	
Flanigan	Mean Value	+1.51%	+0.37%		
	Standard Deviation	±12.30%	±9.09%		
Park	Mean Value		+24.70%		
	Standard Deviation		±10.61		
Sciince	Mean Value				+17.19
	Standard Deviation				±8.31

the curves are extrapolated, they appear to cross at a temperature difference below 100°F. Flanigan (8) observed the intersection at approximately the same temperature difference range for a 0.75 inch O. D. heater boiling in liquid nitrogen. Also, Flanigan (8) observed the same increase in the heat flux at pressures approaching the critical point. Park (13) reported a decrease in the heat flux with increasing pressure near the critical point for both nitrogen and methane.

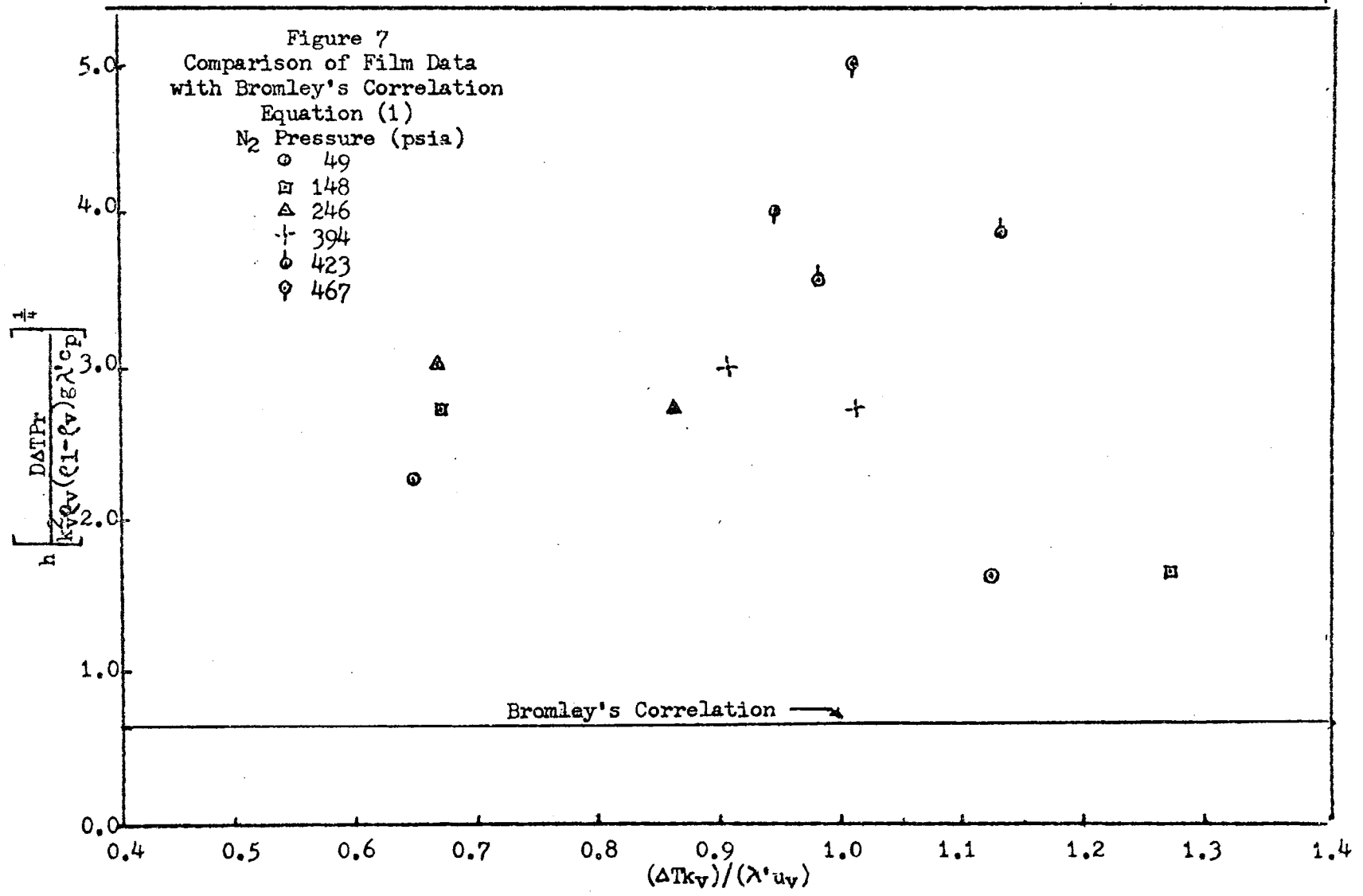
Figure (5) shows that the heat flux in argon increases with increasing pressure until a reduced pressure of 0.80 is reached. The heat flux increases again at a reduced pressure of 0.90. At a reduced pressure of 0.95, the heat flux is approximately the same over the entire temperature difference range as the heat flux of 0.90, and only one line is drawn through these two sets of points. It should be noted that the first three reduced pressure curves (0.1, 0.3, 0.5) were run one month prior to the last three curves (0.8, 0.9, 0.95). A new heat transfer element and thermocouples were used for the last three runs. The greatest percent deviation between the runs of reduced pressures 0.5 and 0.8 is less than 5%. Park (13) reported that the heat loss in film boiling heat transfer can be as high as 4.8%. Therefore, it is difficult to determine whether or not the decrease in heat flux at a reduced pressure of 0.8 is caused by actual boiling behavior or by loss of accuracy. Also, Figure (5) shows no intersection of the pressure curves at temperature differences above 100°F. Flanigan (8) reported a decrease in the heat flux at pressures approaching the critical point of the fluid and he reported an

intersection of the pressure curves at a temperature difference of approximately 125°F when boiling argon with a 0.75 inch heater.

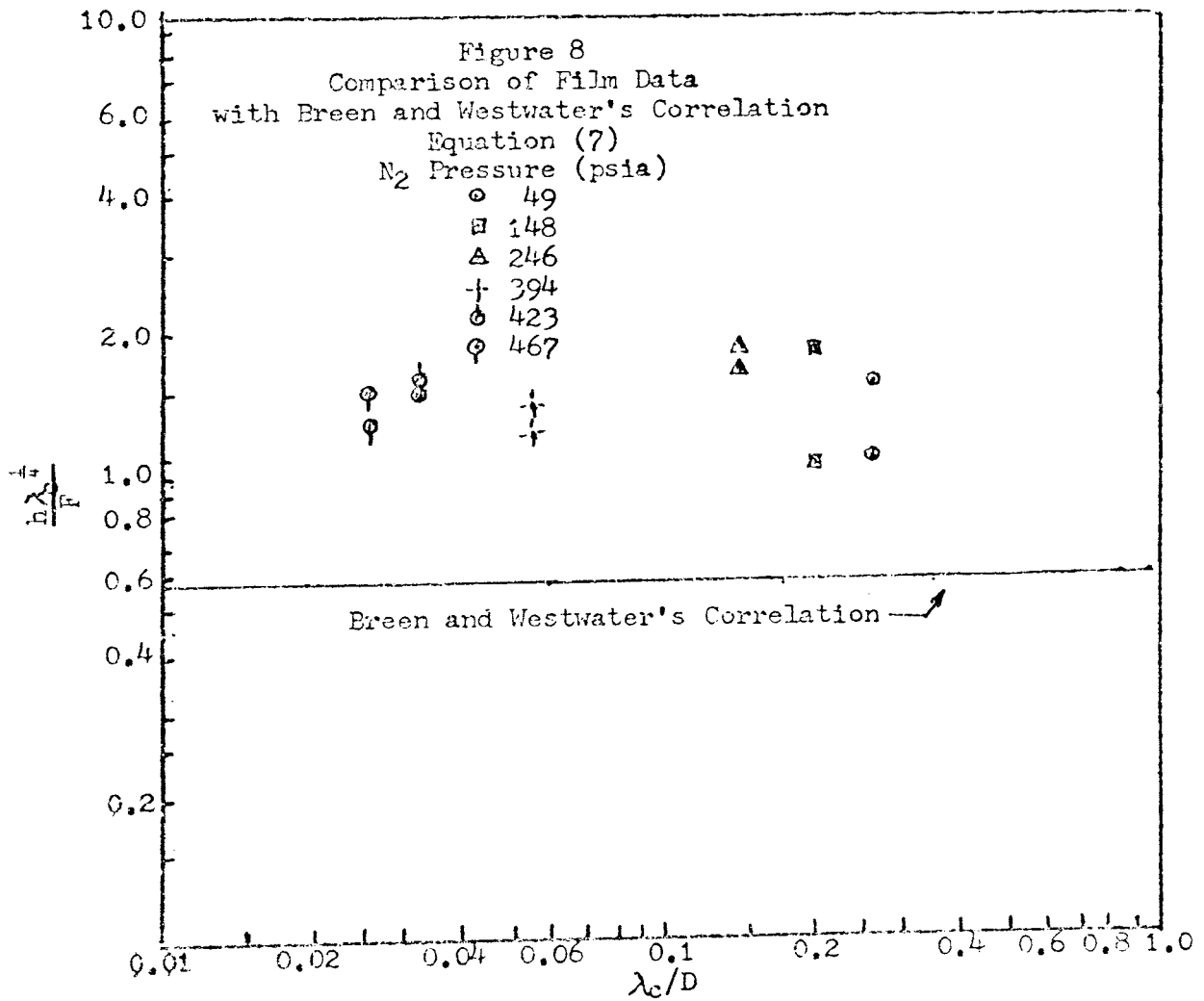
Figure (6) indicates considerable irregularity in the boiling behavior of liquid carbon monoxide. Lines are drawn through the data at reduced pressures of 0.10, 0.50, 0.80, and 0.95. The curves for the reduced pressure curves of 0.30 and 0.90 were not drawn because the lines would lie too close together and would not show any other significant trends in the data. Although the heat flux for the film boiling of carbon monoxide at reduced pressures greater than 0.50 decreases, equation 13 predicts the heat transfer coefficients with a mean deviation of - 3.67% and a standard deviation of $\pm 12.30\%$.

Three heat transfer elements were used in obtaining the data, but the heat flux for film boiling was not significantly affected. The first heating element was used for boiling only nitrogen, the second element was used for boiling both nitrogen and argon, and the third heat transfer element was used for boiling nitrogen, argon and carbon monoxide. Although all the heat transfer surfaces were gold plated, the surfaces of the three heaters were found by Jöhler (11) to be different when in the nucleate boiling region. However, the heat flux for the film boiling of nitrogen, argon, and carbon monoxide reproduced with less than 3% deviation for all three heat transfer elements.

Bromley's correlation (equation 1) and the correlation of Breen and Westwater (equation 7) did not accurately predict the experimental heat transfer data of this investigation. Two data points were chosen at random from each pressure given in Table V for the boiling of nitrogen and were used for the analysis. As shown by Figure 7, the



experimental data are approximately 80% higher than the value predicted by Bromley's correlation (equation 1). The same set of data were used for the analysis of Breen and Westwater's correlation (equation 7). Figure 8 shows the experimental data are approximately 60% higher than the values predicted by equation 7. Also, the data in Figure 8 are located vertically according to the pressure of the system and indicate that equation 7 does not predict the effect of pressure for the film boiling of nitrogen.



CHAPTER VIII

CONCLUSIONS

1. The data of this investigation show that at a given temperature difference in the range from 100 to 500°F, the heat flux increases with increasing pressure for the film boiling of nitrogen and argon from horizontally positioned cylindrical heaters.
2. The data of this investigation show that for the film boiling of carbon monoxide, the heat flux increases with an increase in pressure for reduced pressures up to 0.5 and decreases at a reduced pressure of 0.8. When operating at reduced pressures of 0.90 and 0.95, the heat flux decreased up to a temperature difference of 300°F and increased at temperatures differences greater than 300°F.
3. The least squares approximation (equation 13),

$$h = 255.83 + 94.69(P_r) - 86.79(P_r)^2 + 21.02 (P_r)^3 - 0.3158(\Delta T) + 4.13 \times 10^{-4}(\Delta T)^2 - 438.02(D) + 286.09(D)^2$$
 expressing the heat transfer coefficient as a function of the diameter of the heater, the temperature difference between the surface and the fluid, and the reduced pressure of the system was found to predict the data of this investigation with average deviations of +3.32%, +8.15%, and -3.67% with standard deviations of $\pm 8.81\%$, $\pm 5.55\%$, and $\pm 12.30\%$ for argon, nitrogen, and carbon monoxide, respectively.
4. There were no noticeable effects in the heat flux caused by a change in the surface when different heaters were used.

5. The correlations of Bromley (equation 1), and Breen and Westwater (equation 7) predicted values which were in error by approximately 80% and 60%, respectively.

NOMENCLATURE

A	Area, ft ²
a	Constant in equation 3
a ₁ ...	Constants in equation 12
C	Constant in equations 3 & 8, inches ⁻¹
c _p	Heat Capacity, Btu/lb ^o F
D	Diameter, Ft
E	Potential, volts
F	$(k^3 \rho_v (\rho_l - \rho_v) g \lambda' / \Delta T_u)^{1/4}$, Btu/HrFt ^{2o} F
g	Acceleration due to gravity, ft/sec ²
g _c	Gravitational Constant, lb _m ft/lb _f sec ²
Gr*	Generalized Grashof Number
h	Heat Transfer coefficient, Btu/HrFt ^{2o} F
I	Current, amp
k	Thermal Conductivity, Btu/HrFt ^{2o} F/Ft
L	Length, Ft
M	Molecular Weight, lb/lb-mole
Nu*	Generalized Nusselt Number
P	Pressure, psi
P _r	Reduced Pressure, P/P _c
Pr ¹	Prandtl Number
Pr*	Generalized Prandtl Number
Q	Rate of heat transfer, Btu/Hr
T	Temperature, °R
T	Temperature Difference (T _{surface} - T _{fluid}), °F or °R
v	Specific volume, ft ³ /lb
W	Maximum vapor mass flow rate, lb _m /sec

Greek Symbols

σ	Surface Tension, lb/ft
λ_c	$(g/g_c(\rho_l - \rho_v))^{1/2}$, ft
μ	Viscosity, lb/ft hr
ρ	Density, lb/ft ³
α	Equivalent Thermal Diffusivity, ft ² /hr
γ	Kinematic Viscosity, ft ² /hr
λ	Latent Heat of Vaporization, Btu/lb _m
λ'	Latent Heat of Vaporization Plus Average Sensible Heat Content of Vapor, Btu/lb _m
θ	Temperature difference, °R

Subscripts

c	refers to the critical point
v	refers to the vapor
l	refers to the liquid
r	refers to reduced property, (T/T _c , etc.)

BIBLIOGRAPHY

1. Berenson, P. J., "Film Boiling Heat Transfer from a Horizontal Surface", J. Heat Transfer, Vol. 83, 1961, P. 351.
2. Banchemo, J. T., Barker, G. E., and Boll, R. H., "Stable Film Boiling of Liquid Oxygen Outside Single Horizontal Tubes and Wires", Heat Transfer, Chemical Engineering Progress, Symposium Series, Vol. 51, No. 17, American Institute of Chemical Engineers, New York, 1965, P. 21.
3. Breen, B. P. and Westwater, J. W., "Effect of Diameter of Horizontal Tubes on Film Boiling Heat Transfer", Chem. Eng. Prog., Vol. 58, July 1962, P. 67.
4. Bromley, L. A., "Heat Transfer in Stable Film Boiling", Chem. Eng. Prog., Vol. 46, May 1950, P. 221.
5. Bromley, L. A., "Effect of Heat Capacity of Condensate", Industrial and Engineering Chemistry, Vol. 44, December 1952, P. 2966.
6. Chang, Y. P., "Wave Theory of Heat Transfer in Film Boiling", J. Heat Transfer, Vol. 1, January 1959, P. 1.
7. Farber, E. A. and Scoria, R. L., "Heat Transfer to Water Boiling Under Pressure", Trans. Am. Soc. Mech. Eng., May 1948, P. 369.
8. Flanigan, J. J., Jr., "A Study of Film Boiling of Liquid Nitrogen and Liquid Argon Over a Wide Pressure Range with Cylinder Heaters" Ph.D. Thesis, University of Missouri at Rolla, 1967.
9. Guggenheim, E. A., Thermodynamics, North-Holland Publishing Co., Amsterdam, 1959.
10. Jakob, M., Heat Transfer, Vol. 1, John Wiley & Sons, Inc., New York, 1949.
11. Johler, C. B., M.S. Thesis, University of Missouri at Rolla, 1968.
12. Nukiyama, S. J., Soc. Mech. Engr's. (Japan), Vol. 37, 1931, P. 367.
13. Park, E. L., Jr. "Nucleate and Film Boiling Heat Transfer to Methane and Nitrogen from Atmospheric to the Critical Pressure", Ph.D. Thesis, University of Oklahoma, 1965.
14. Perry, J. H., Chemical Engineer's Handbook, McGraw-Hill Company, Inc., New York, 1963.
15. Pitzer, K. S., "Corresponding States for Perfect Liquids", J. Chem. Phys., Vol. 7, Aug. 1939, P. 583.

16. Sciance, C. T., Ph.D. Thesis, University of Oklahoma, 1966.
17. Stranberg, R. M., Jr., Computer Science Center, University of Missouri at Rolla, Personal communication.

APPENDICES

APPENDIX A
DISCUSSION OF ERRORS

Park (13) discussed the error introduced by neglecting heat loss at the ends of cylindrical heat transfer elements of the type used in this investigation. He reports the end losses to be approximately 4.8%. An estimate of the end losses was made for the first data point of Table 5 (N₂ data). The heat transfer from the walls of the heater was 25 times the heat transfer from the ends and the end loss of 4% was a conservative estimate. Banchemo, Barker, and Boll (2) found experimentally that for cylindrical heaters with the dimension used in this investigation the axial temperature gradient were virtually eliminated.

The current and the voltage supplied to the heater was read accurately within ± 0.1 amps and ± 0.01 volts, respectively. At the minimum values of voltage (5 volts) and of amperage (10 amps), the maximum error in an experimentally determined heat flux was 1.2%. The thermocouples were read to ± 0.001 millivolts, which corresponds to $\pm 0.047^\circ\text{F}$. This degree of precision is attributed to the use of digital voltmeters and the use of silver solder in securing the thermocouple junctions and in filling the thermocouple wells in the walls of the heater. The temperature gradient around the heat transfer element was no larger than 6°F . At lower values of temperature difference (150°F), this temperature gradient could contribute an additional 4% error. The pressure was read to ± 1 pound per square inch and at a reduced pressure of 0.1 for nitrogen (33 psig) the maximum error was approximately 3%. Therefore, a conservative estimate of the total error in the heat flux introduced by the above experimental limitations was 9%.

APPENDIX B
Sample Calculations

A. Sample Calculations for the first data point of Table 5 Data:

$$E = 12.78 \text{ volts}$$

$$I = 11.2 \text{ amps}$$

$$\Delta T = 179.0^\circ\text{F}$$

$$A = 0.049 \text{ ft}^2$$

1. Calculation of the heat flux

$$Q/A = 3.414 \text{ Btu/watt-hr } (E) (I)/(A) = 0.993 \text{ Btu/hr-ft}^2 \times 10^{-4}$$

2. Calculation of the heat transfer coefficient

$$h = 0.993 \text{ Btu/hr-ft}^2 / 179.0^\circ\text{F} = 55.4 \text{ Btu/hr-ft}^2\text{-}^\circ\text{F} = Q/A \Delta T$$

3. Calculation of the heat transfer coefficient predicted from Equation 13 in Chapter VII

$$h = 53.6 \text{ Btu/hr-ft}^2\text{-}^\circ\text{F}$$

where $D = 0.75 \text{ inches}$

$$Pr = 0.10$$

$$\Delta T = 179.0^\circ\text{F}$$

4. Calculation of the percent deviation

$$\text{Percent Deviation} = 55.4 - 53.6 / 55.4 \times (100) = 3.30\%$$

B. Sample Calculation Using Bromley's Correlation (equation 1)

N_2 Operating Conditions For Second Data Point of Table 5

$$\text{Pressure} = 49 \text{ psia}$$

$$T_{\text{sat}} = -180.5^\circ\text{C}$$

$$\Delta T = 211^\circ\text{F}$$

$$\text{Average Film Temperature} = 277^\circ\text{R}$$

$$h = 52.6 \text{ Btu/hr ft}^2\text{-}^\circ\text{F}$$

$$D = 0.75 \text{ inches}$$

Fluid Properties:

$$\sigma = 33.8 \times 10^{-5} \text{ lb/ft (reference 13)}$$

$$\mu_v = 0.0244 \text{ lb/ft hr (reference 13)}$$

$$k_v = 0.0080 \text{ Btu/hrft}^{2\circ\text{F}}/\text{ft (reference 13)}$$

$$\lambda = 78.4 \text{ Btu/lb}_m \text{ (reference 14)}$$

$$\rho_v = 0.094 \text{ lb}_m/\text{ft}^3 \text{ (reference 14)}$$

$$\rho_l = 46.9 \text{ lb}_m/\text{ft}^3 \text{ (reference 14)}$$

$$c_p = 0.257 \text{ Btu/lb}_m^{\circ\text{F}} \text{ (reference 14)}$$

1. Calculation of $\lambda\rho$

$$\lambda'' = \lambda \left[1 + (0.34 c_p \Delta T) / \lambda \right]^2 = 119.9 \text{ Btu/lb}_m$$

2. Calculation of value for the Ordinate of Figure 7

$$h = \left[\frac{D \Delta T \mu_v}{k_v^3 \rho_v (\rho_l - \rho_v) g \lambda''} \right]^{\frac{1}{4}} = 2.31 \text{ Btu/hr-ft}^{2-\circ\text{F}}$$

3. Calculation of Value for the Abscissa of Figure 7

$$\frac{\Delta T k_v}{\lambda'' \mu_v} = 0.645$$

- C. Calculation Using Breen and Westwater's Correlation (equation 7) for the same data point

1. Calculation of Critical Wavelength

$$\lambda_c = 2\pi \left[\frac{\sigma}{\rho_l - \rho_v} \right]^{\frac{1}{2}} = 0.01681 \text{ ft}$$

2. Calculation of Value for the Ordinate of Figure 8

$$F = \left[\frac{k_v^3 \rho_v (\rho_l - \rho_v) g \lambda''}{\mu_v \Delta T} \right]^{\frac{1}{4}} = 12.2 \text{ Btu/hr-}^{\circ\text{F}}\text{-ft}^{\frac{3}{4}}$$

$$h \lambda_c^{\frac{1}{4}} / F = 1.66$$

3. Calculation of Value for the Abscissa of Figure 8

$$\lambda_c / D = 0.269$$

APPENDIX C
Calculated Data

on of film boiling heat transfer coefficients for cylinder
 squares approximation.

duced pressure of fluid at the saturation temperature, P/P_c

eter of cylinder in inches

temperature difference between surface and fluid, $^{\circ}\text{F}$

perimental heat transfer coefficients, $\text{Btu/hr ft}^2\text{ }^{\circ}\text{F}$

= Heat transfer coefficients by least squares approximation,
 $\text{Btu/hrft}^2\text{ }^{\circ}\text{F}$

xperimental Heat Flux, $\text{Btu/hrft}^2 \times 10^{-4}$

Table II

Flannigan Ph.D. Thesis - Nitrogen Data

D	Delt	H	Calc H	% Error
0.55	352.3	52.2	50.1	4.11
0.55	258.0	72.4	68.6	5.21
0.55	269.5	72.7	74.6	-2.58
0.55	200.5	77.9	85.7	-10.07
0.55	170.0	81.8	89.9	-10.01
0.55	171.0	83.6	89.1	-6.59
0.75	328.3	43.6	37.7	13.44
0.75	316.00	55.1	50.8	7.65
0.75	276.0	63.2	60.8	3.82
0.75	262.0	67.6	64.8	4.06
0.75	124.0	85.3	85.7	-0.42
0.75	158.0	77.3	78.3	-1.19
0.95	324.3	41.1	47.6	-15.81
0.95	232.5	73.6	68.0	7.58
0.95	230.5	77.0	75.3	2.18
0.95	236.0	78.8	77.3	1.85
0.95	176.5	85.0	85.3	-0.34
0.95	211.2	82.4	79.3	3.85

Argon Data

0.55	199.0	69.1	63.6	7.97
0.55	309.0	73.8	64.5	12.64
0.55	177.5	102.2	86.7	15.23
0.55	192.0	127.6	87.0	31.81
0.55	206.0	73.1	84.2	-15.11

Table II continued

Pr	D	Delt	H	Calc H	% Error
0.955	0.55	180.0	82.9	87.6	-5.59
0.10	0.75	212.0	47.9	48.5	-1.26
0.30	0.75	274.0	56.9	53.9	5.36
0.50	0.75	142.0	74.3	80.0	-7.66
0.80	0.75	212.0	76.7	70.8	7.68
0.90	0.75	192.00	68.3	73.1	-6.95
0.955	0.75	233.0	73.4	66.7	9.16
0.10	0.95	195.5	62.8	60.6	3.54
0.30	0.95	165.5	80.4	78.1	2.79
0.50	0.95	175.0	85.7	83.6	2.51
0.80	0.95	185.0	79.7	84.6	-6.16
0.90	0.95	175.0	70.1	85.5	-22.04
0.955	0.95	180.0	78.8	84.0	-6.60

Table III

Park Ph.D. Thesis - Nitrogen Data

Pr	D	Delt	H	Calc H	% Error
0.233	0.8022	154.0	106.1	67.3	36.54
0.233	"	210.0	87.3	58.1	33.49
0.300	"	218.0	90.0	60.5	32.78
0.300	"	275.0	76.90	54.1	29.64
0.437	"	238.0	83.6	63.3	24.23
0.610	"	233.0	81.2	67.6	16.71
0.795	"	226.0	81.2	69.3	14.70
0.902	"	174.0	27.3	76.3	-179.62
0.300	"	143.0	112.4	73.0	35.05
0.437	"	144.0	108.7	78.2	28.06
0.610	"	325.0	75.5	59.8	20.83
0.795	"	126.0	93.7	86.3	7.89
0.795	"	172.0	86.1	77.4	10.06
0.795	"	313.0	76.2	61.2	19.74
0.795	"	81.0	114.6	96.7	15.65
0.610	"	54.0	192.6	102.9	46.55
0.902	"	256.0	27.3	65.0	-138.10
0.437	"	337.0	72.5	55.6	23.33

Table IV

Science Ph.D. Thesis - Methane Data

Pr	D	Delt	H	Calc H	% Error
0.90	0.811	52.0	126.9	103.7	18.28
0.90	"	157.0	102.5	79.6	22.33
0.90	"	285.0	95.4	62.5	34.43
0.80	"	74.0	120.0	98.6	17.82
0.80	"	183.0	96.7	75.8	21.65
0.80	"	411.0	86.1	59.7	30.66
0.30	"	230.0	67.8	59.1	12.78
0.20	"	297.0	66.3	47.0	29.06
0.20	"	269.0	58.4	49.3	15.53
0.40	"	216.0	72.6	65.1	10.27
0.50	"	201.0	77.1	70.2	8.90
0.60	"	187.0	85.0	74.3	12.64
0.70	"	149.0	86.5	81.8	5.39
0.70	"	200.0	82.5	73.1	11.42
0.80	"	140.0	90.0	83.6	7.10
0.80	"	199.0	86.3	73.2	15.13
0.90	"	109.0	102.0	89.5	12.26
0.90	"	209.0	93.3	71.0	23.85

Table V

Capone Nitrogen Data - 0.75" O. D. Heater

Pr	Q/A	Delt	H	Calc H	% Error
0.10	0.993	179.0	55.4	53.6	3.30
0.10	1.111	211.0	52.6	48.6	7.56
0.10	1.259	270.0	46.8	41.7	10.87
0.10	1.305	284.0	45.9	40.5	11.78
0.10	1.350	303.0	44.6	39.1	12.34
0.10	1.481	341.0	43.4	37.2	14.27
0.10	1.560	359.0	43.4	36.7	15.38
0.10	1.680	392.0	43.0	36.5	15.03
0.10	1.892	438.0	43.0	37.8	12.14
0.30	2.650	452.0	58.7	51.0	13.06
0.30	2.460	436.0	56.4	50.2	10.96
0.30	2.380	420.0	56.8	49.6	12.65
0.30	2.040	361.0	56.4	49.2	12.74
0.30	1.635	270.0	60.9	54.2	10.94
0.30	1.401	225.0	62.6	59.3	5.35
0.30	1.261	191.0	66.1	64.1	2.95
0.30	1.615	295.0	54.7	52.2	4.61
0.30	1.912	326.0	59.1	50.3	14.82
0.50	1.899	316.0	60.1	58.0	3.57
0.50	1.986	328.5	60.4	57.3	5.08
0.50	2.130	358.5	59.4	56.4	5.10
0.50	2.260	385.0	58.9	56.1	4.69
0.50	2.340	401.0	58.3	56.3	3.46
0.50	2.550	435.0	58.5	57.3	2.08
0.50	1.822	295.5	61.8	59.2	4.13
0.50	1.639	256.0	64.0	62.7	1.99
0.50	1.435	216.0	66.5	67.6	-1.60
0.50	1.269	176.0	72.1	73.7	-2.24
0.50	1.219	144.0	84.5	79.6	5.81
0.80	1.253	160.9	78.0	79.1	-1.39
0.80	1.381	181.0	76.3	75.6	0.95
0.80	1.581	218.3	72.5	69.9	3.52
0.80	1.812	258.2	70.1	65.2	6.99
0.80	1.945	282.0	69.1	63.0	8.84
0.80	2.130	310.0	68.9	61.0	11.47
0.80	2.375	354.0	67.1	59.2	11.82
0.80	2.640	402.0	65.8	59.0	10.34
0.80	2.840	437.0	65.0	60.1	7.58
0.80	1.885	275.0	68.6	63.6	7.30
0.86	1.022	121.0	84.0	86.5	-2.97
0.86	1.238	157.9	78.5	79.3	-1.00
0.86	1.490	201.0	74.3	72.1	3.01
0.86	1.699	238.5	71.4	67.0	6.13
0.86	1.961	280.0	70.3	62.8	10.66
0.86	2.160	311.0	69.4	60.6	12.70
0.86	2.360	349.0	67.8	58.9	13.07

Table V continued

Pr	Q/A	Delt	H	Calc H	% Error
0.86	2.650	380.0	67.1	58.5	12.84
0.86	2.810	433.0	64.9	59.5	8.25
0.95	1.165	137.0	85.1	82.4	3.19
0.95	1.680	220.0	76.4	68.4	10.46
0.95	2.110	287.0	73.5	61.3	16.63
0.95	2.370	325.0	73.0	58.9	19.34
0.95	2.590	362.0	71.5	57.7	19.30
0.95	2.720	386.0	70.5	57.5	18.40

Argon Data

0.10	0.846	193.0	43.9	51.3	-16.86
0.10	1.119	262.0	42.7	42.5	0.52
0.10	1.792	409.0	43.9	36.8	16.19
0.10	2.000	447.0	44.8	38.2	14.67
0.10	0.772	151.8	47.6	58.4	-22.79
0.10	0.985	228.0	43.1	46.3	-7.51
0.10	1.275	303.0	42.1	39.1	7.13
0.10	1.421	325.0	43.8	37.9	13.57
0.10	1.625	358.0	45.4	36.7	19.07
0.10	1.919	438.0	43.8	37.8	13.74
0.30	0.976	138.0	70.6	73.7	-4.37
0.30	1.375	221.0	62.2	59.8	3.89
0.30	1.610	276.0	58.4	53.7	8.05
0.30	2.000	345.0	58.5	49.6	15.21
0.30	0.817	105.9	77.2	80.6	-4.39
0.30	1.210	188.0	64.5	64.6	-0.19
0.30	1.490	249.0	59.9	56.4	5.89
0.30	1.790	309.0	58.0	51.2	11.64
0.30	2.180	389.0	56.1	49.0	12.57
0.30	2.360	723.0	55.9	49.7	11.07
0.50	1.711	224.0	76.5	66.5	13.09
0.50	1.901	289.0	65.9	59.7	9.36
0.50	2.190	335.0	65.4	57.1	12.75
0.50	2.500	392.0	64.0	56.2	12.23
0.50	1.310	178.0	73.5	73.4	0.16
0.50	1.802	137.0	79.0	81.0	-2.39
0.50	1.778	267.0	66.7	61.6	7.60
0.50	2.040	312.0	65.5	58.2	11.18
0.50	2.360	362.0	65.3	56.3	13.77
0.50	1.522	218.0	70.0	67.3	3.87
0.80	1.279	180.0	71.2	75.7	-6.38

Table V continued

Pr	Q/A	Delt	H	Calc H	% Error
0.80	1.399	215.0	65.0	70.4	-8.31
0.80	1.511	242.0	62.5	67.0	-7.15
0.80	1.718	264.0	65.0	64.6	0.59
0.80	1.993	314.0	63.4	60.8	4.16
0.80	2.200	346.0	63.2	59.4	6.04
0.80	2.320	372.0	62.4	58.9	5.64
0.80	1.340	189.0	71.0	74.3	-4.61
0.80	1.183	159.0	74.4	79.4	-6.77
0.80	0.964	122.0	78.7	86.8	-10.32
0.90	1.300	172.0	75.6	76.4	-1.04
0.90	1.480	202.0	73.1	71.5	2.13
0.90	1.550	215.0	72.1	69.7	3.36
0.90	1.730	246.0	70.3	65.8	6.41
0.90	1.922	280.0	68.6	62.4	8.98
0.90	2.085	326.0	64.0	59.4	7.15
0.90	2.285	366.0	62.5	58.2	6.84
0.90	1.180	156.0	75.4	79.3	-5.13
0.90	1.020	128.0	79.5	84.8	-6.70
0.95	0.750	80.0	93.8	95.3	-1.57
0.95	0.935	110.0	85.0	88.2	-3.71
0.95	1.239	157.0	79.0	78.5	0.64
0.95	1.519	208.0	71.9	70.1	2.54
0.95	1.735	244.0	71.0	65.4	7.85

Carbon Monoxide Data

0.10	1.165	252.0	46.2	43.5	5.81
0.10	1.328	293.0	45.3	49.8	12.15
0.10	1.441	327.0	44.0	37.8	14.17
0.10	1.663	384.0	43.4	36.5	15.90
0.10	1.815	428.0	42.5	37.4	12.09
0.10	1.960	464.0	42.3	39.3	7.20
0.10	2.040	481.0	42.4	40.5	4.66
0.10	1.501	358.0	42.0	36.7	12.51
0.10	0.990	214.0	46.2	48.2	-4.33
0.30	1.311	181.0	72.4	65.8	9.16
0.30	1.469	240.0	61.2	59.3	3.11
0.30	1.610	280.0	57.4	53.4	7.05
0.30	1.759	314.0	56.1	51.0	9.17
0.30	1.912	355.0	53.4	49.3	7.61
0.30	2.130	405.0	52.6	49.2	6.38
0.30	2.320	454.0	51.2	51.2	-0.10
0.30	1.459	282.0	51.7	53.2	-2.87
0.30	1.293	242.0	53.5	57.2	-6.84
0.30	1.098	193.0	57.0	63.8	-11.99
0.50	1.462	175.0	84.4	73.0	12.45
0.50	1.581	228.0	69.4	66.0	4.94

Table V continued

Pr	Q/A	Delt	H	Calc H	% Error
0.50	1.692	268.0	63.1	61.5	2.48
0.50	1.893	318.0	59.6	57.8	2.94
0.50	2.100	368.0	57.0	56.2	1.37
0.50	2.285	416.0	55.0	56.6	-2.92
0.50	2.380	449.0	53.6	58.0	-8.16
0.50	1.695	300.0	56.5	58.9	-4.31
0.50	1.582	273.0	58.0	61.1	-5.30
0.80	1.032	91.2	113.2	93.8	17.10
0.80	1.250	209.0	59.9	71.2	-18.94
0.80	1.399	246.0	56.9	66.5	-16.89
0.80	1.635	300.0	54.5	61.6	-13.09
0.80	1.818	339.0	53.6	59.6	-11.21
0.80	1.945	366.0	53.1	58.9	-11.01
0.80	2.060	394.0	52.5	58.9	-12.17
0.80	2.28	426.0	53.5	59.6	-11.45
0.80	1.128	210.0	53.4	71.1	-33.14
0.90	0.864	144.0	60.2	81.6	-35.50
0.90	1.061	180.0	59.1	75.0	-26.94
0.90	1.258	218.0	57.7	69.3	-20.05
0.90	1.425	252.0	56.6	65.1	-15.07
0.90	1.652	298.0	55.5	61.1	-10.00
0.90	1.864	341.0	54.8	58.8	-7.34
0.90	2.015	372.0	54.5	58.2	-6.71
0.90	2.200	405.0	54.3	58.3	-7.42
0.90	1.300	222.0	58.5	68.7	-17.49
0.95	0.881	131.0	67.2	83.6	-24.42
0.95	1.188	185.0	64.3	73.6	-14.47
0.95	1.421	231.0	61.5	67.0	-8.92
0.95	1.542	252.0	61.3	64.5	-5.28
0.95	1.701	280.0	60.9	61.8	-1.56
0.95	1.845	305.0	60.5	60.0	0.84
0.95	1.972	326.0	60.5	58.8	2.75
0.95	2.045	394.0	61.1	57.6	5.76

Additional Nitrogen Data

0.95	1.459	183.0	79.7	74.5	6.52
0.95	1.955	264.0	74.1	63.9	13.78
0.95	2.900	417.0	67.0	58.8	12.22

Additional Argon Data

0.95	2.040	299.0	68.0	60.9	10.42
0.95	2.270	344.0	65.8	59.0	10.32
0.95	2.500	387.0	64.5	58.2	9.77
0.95	1.862	255.0	72.6	64.9	10.60

APPENDIX D
Operating Conditions

Table VI
Operating Conditions

Nitrogen: $P_c = 490$ psia, $T_c = -147^\circ\text{C}$

Solute Pressure psia	Reduced Pressure P_r	Saturation Temperature $T_{\text{sat}} \text{ }^\circ\text{C}$
49	0.10	-180.5
148	0.30	-166.3
246	0.50	-158.6
394	0.80	-149.4
423	0.86	-148.4
467	0.95	-146.4

Argon: $P_c = 480$ psia, $T_c = -122^\circ\text{C}$

71	0.10	-165.0
198	0.30	-147.5
352	0.50	-137.4
564	0.80	-125.5
634	0.90	-122.6
670	0.95	-121.2

Carbon Monoxide: $P_c = 510$ psia, $T_c = -139^\circ\text{C}$

36	0.10	-175.7
138	0.30	-160.5
239	0.50	-151.9
392	0.80	-143.0
446	0.90	-140.4
467	0.95	-139.6

147520

VITA

Gary Joseph Capone, son of Mr. and Mrs. Marion J. Capone, was born at St. Elizabeth Hospital in Belleville, Illinois on August 20, 1935.

He attended Belleville Township High School and graduated in June, 1963. He was admitted to the University of Missouri - Rolla in September of 1963 and received his Bachelor of Science degree in Chemical Engineering in May of 1967. In September of 1967 he returned to the University to begin work on a Master of Science degree in Chemical Engineering.